Building and Environment 281 (2025) 113208

Contents lists available at ScienceDirect

Building and Environment

journal homepage: www.elsevier.com/locate/buildenv

TiO_2-P25 Enhanced Thermochromic Coatings for Energy Efficient Roofing: Evaluating Long-Term Performance through Accelerated Aging Tests

Ana Carolina Hidalgo-Araujo [a,c], Rafael Salomão [b], Umberto Berardi [c,d], Kelen Almeida Dornelles [a]

[a] Institute of Architecture and Urbanism, University of São Paulo (USP), Brazil
[b] São Carlos School of Engineering, Materials Engineering Department, USP, Brazil
[c] Architectural Science, Toronto Metropolitan University, TMU, Toronto, Canada
[d] Department of Civil Engineering and Architectural Sciences, Politecnico di Bari, Italy

ARTICLE INFO

Keywords:
Adaptive materials
Accelerated aging testing
Energy efficiency
Laboratory testing
Building envelope
Building energy simulation
Climate adaptation

ABSTRACT

As global warming intensifies, passive cooling strategies are critical in reducing energy consumption, mitigating the urban heat island effect, and reducing greenhouse gas emissions. This study investigates the energy performance and durability of thermochromic coatings applied to ceramic and fiber cement roof tiles in two climatically different Brazilian cities: Manaus (humid equatorial) and Curitiba (subtropical). The coatings of microencapsulated organic pigments combined with rutile TiO_2 were enhanced with colloidal silica (SiO_2) and anatase TiO_2-P25 nanoparticles to improve long-term stability. Accelerated aging tests were performed according to ASTM D7897, and solar reflectance was measured according to ASTM E903 and G173. This data was incorporated into EnergyPlus simulations under projected climate conditions for 2050. Simulation results showed that lowering the pigment's transition temperature (TT) to 20 °C significantly improved energy performance in subtropical climates. In Curitiba, thermochromic roof coatings reduced energy consumption by up to 7.3% in unaged and 5.2% in aged samples compared to the ceramic roof reference. However, savings could reach 11.3% with improved optical contrast between the two-color states of the pigment. Adding a TiO_2-P25 protective layer effectively reduced pigment degradation, as evidenced by solar reflectance losses that were approximately 50.4% lower below the TT and 33.3% lower above the TT, compared to unprotected samples. These results highlight the potential of thermochromic coatings to improve the energy efficiency of buildings in climates with significant temperature variations and underscore the need for tailored formulations. The study also calls for region-specific accelerated aging protocols, natural weathering testing, and further research to enhance color contrast and reduce photodegradation to improve the durability and reliability of thermochromic pigments.

1. Introduction

As global warming continues to affect energy consumption in buildings, research into passive strategies to reduce dependence on artificial climate control is essential to decrease greenhouse gas emissions and mitigate the urban heat island effect [1]. One promising solution involves materials with adaptive optical properties, such as organic thermochromic pigments, which are considered the third generation of cool materials [2,3]. Based on reversible chemical reactions, these microencapsulated systems consist of a color former (*leuco* dye), a color developer, and a solvent [4]. At a specific TT, the materials undergo a color change that modifies their ability to reflect solar radiation [5]. In warmer conditions, solar reflectance increases to reduce heat absorption, while in cooler conditions, it decreases to retain heat [6].

This adaptive behavior helps overcome the winter penalty associated with traditional cool materials, enhancing thermal regulation throughout the year and reducing reliance on artificial heating and cooling [7,8]. Studies have demonstrated significant energy savings achieved through the use of thermochromic coatings: Soudian et al. [9] showed that adding thermochromic paint and phase change materials to cementitious plaster increases solar reflectance by 23 % and dynamically regulates solar absorption. Berardi et al. [10] found that applying thermochromic paint to facades reduced cooling demand by 8.9 % while limiting winter heating penalties to just 1.7 % in Toronto, Canada. Yuxuan et al. [11] reported savings of 4.28-5.02 kWh/m^2 with thermochromic coatings. Similarly, Sánchez et al. [12] observed a 1-12 % reduction in annual energy demand. Khaled et al. [13] found that combining exterior thermochromic and interior low-e glazing reduced annual energy use by up to 12 kWh/m^2 in Abu Dhabi and 6.3 kWh/m^2 in

https://doi.org/10.1016/j.buildenv.2025.113208
Received 19 February 2025; Received in revised form 15 May 2025; Accepted 20 May 2025
Available online 21 May 2025

Nomenclature

TC	Thermochromic coating
TC+P25	Thermochromic coating with the TiO_2-P25 protective layer
TT	Transition Temperature
DSC	Differential Scanning Calorimetry
UV	Ultraviolet
VIS	Visible
IR	Infrared
ρ	Solar Reflectance
α	Solar Absorptance
EMS	Energy Management System
IDF	Input Data File
PCM	Phase Change Material
CFD	Computational Fluid Dynamics
UCM	Urban Canopy Model
MCMV	*Minha Casa Minha Vida*
TMY	Typical Meteorological Years
t	Thickness
λ	Thermal conductivity
ρ	Density
c	Specific heat capacity
CLG	Cooling Load
HTG	Heating Load

Toronto.

More recently, Song et al. [14] reported 17.8–43.0 MJ/m^2 lower energy use and 9.4–38.0 kg CO_2/m^2 fewer emissions compared to asphalt roofs, using a temperature-adaptive radiative cooling coating based on thermochromic powder. Guo et al. [15] found a 20.3 % energy savings using thermochromic hydrogels, while maintaining surface temperatures 7-10 °C lower than conventional coatings. Azevedo et al. [16] recommended thermochromic coatings for schools in Brazil to optimize comfort in all climates, and Kitsopoulou et al. [17] reported energy savings of 2.19-17.13 % in Athens, Greece, with the highest reductions during the cooling season.

Despite the promising potential of thermochromic coatings, their stability and durability challenges remain significant. Hakami et al. [2] reviewed microencapsulated organic thermochromic materials, recognizing their potential for energy-efficient designs and highlighting their vulnerability to photodegradation. Studies have focused on assessing the aging performance of these materials, with important implications for their long-term use in building applications. Ma et al. [18] were among the first to study the effects of aging on thermochromic coatings, demonstrating that while the coatings did not exhibit problems such as cracking, peeling, or significant changes in color TT after accelerated aging tests, the fading of thermochromic dyes represented a significant durability challenge. Similarly, Sharma et al. [19] observed that although thermochromic elastomeric roof coatings initially performed well, their durability was compromised by irreversible photodegradation after accelerated weathering. Badino et al. [20] reported that thermochromic coatings can reduce surface temperatures by up to 35 °C, but they lose their thermochromic properties after only three days of natural exposure.

The influence of TT on energy demand has also been a research focus. Studies have demonstrated that materials with low TT, such as those developed by Xi et al. [21] and Sun et al. [22], have considerable potential to reduce energy consumption, especially in midlatitude climates. However, the durability of these materials over time is often a crucial factor in determining their long-term effectiveness. While some studies, such as those by Soudian et al. [23], suggested that integrating phase change materials (PCMs) with thermochromic pigments could enhance both durability and solar reflectance, others, like Liu et al. [24], highlighted challenges posed by environmental stressors such as UV exposure and corrosion. Thus, while thermochromic materials show significant promise in enhancing energy efficiency, the aging process and TT remain key factors in determining their practical application and long-term viability.

To address these challenges, some studies have focused on incorporating additives like silicon dioxide (SiO_2) and titanium dioxide (TiO_2) to improve the stability and longevity of thermochromic pigments. SiO_2, known for its high stability, water resistance, and chemical durability, is considered an ideal additive for enhancing the durability of thermochromic coatings [25]. TiO_2, with its photocatalytic properties, exists in two main crystalline forms: anatase, which is particularly effective at decomposing organic pollutants under UV light, and rutile, the more stable form [26]. The TiO_2-P25 grade, a mixture of approximately 75 wt % anatase and 25 wt % rutile, combines photocatalytic activity with superior durability [27].

Hu et al. [6] investigated thermochromic coatings enhanced with TiO_2 nanoparticles, achieving up to 7.7 % energy savings, a 3.6 % reduction in costs, and 28.5 % lower CO_2 emissions compared to conventional cool roofs. In another study, Hu et al. [28] developed PVC-based films incorporating thermochromic dyes and TiO_2 nanoparticles, reducing internal surface temperatures by 3.5 °C on concrete roofs and 9-10 °C on plastic roofs. Liu et al. [24] proposed superhydrophobic thermochromic coatings to save up to 6.76 % of energy in cities with cold winters and hot summers. Simulations in Nanjing and Shanghai showed annual savings ranging from 4.52 % to 6.76 %. Hussain et al. [29] found that SiO_2-coated *leuco* dye-based thermochromic pigments improved hydration, compressive strength, and color stability in Portland cement pastes, with the SiO_2 coating protecting the pigment in harsh conditions. Cheng et al. [30] developed thermochromic superhydrophobic coatings with self-cleaning properties, achieving 13.74 % energy savings in northern China and maintaining functionality after mechanical, chemical, and UV stress. Li et al. [31] synthesized thermochromic phase-change microcapsules, achieving high thermal conductivity and heat storage properties, with a 132.4 % increase in thermal conductivity after adding SiO_2 shells. Despite these promising advancements, research to enhance the long-term performance of microencapsulated thermochromic materials remains limited [32].

To better understand and develop more durable materials, accelerated aging tests provide a valuable approach for evaluating the long-term behavior of building components. Berardi et al. [33] and Berardi [34] evaluated insulation materials by calculating acceleration factors to correlate laboratory weathering with real-world conditions and to estimate the required exposure time in a weathering apparatus simulating heating, humidity, and UV radiation cycles. Couto [35] applied ASTM D7897 [36], which replicates three years of natural weathering for roof tiles using heating, humidity, and UV radiation cycles with the addition of a spraying step to simulate particulate deposition.

In this study, ASTM D7897 [36] was used to evaluate the impact of artificial weathering on the solar reflectance of an organic thermochromic coating, as it is the only standard that provides specific procedures for simulating the aging process of roofing materials. While most studies improve durability by adding either silicon dioxide (SiO_2) or titanium dioxide (TiO_2), this work adopts a combined approach using both additives in a single formulation. Moreover, its main innovation lies in applying a photocatalytic titanium dioxide (TiO_2-P25) protective layer designed to shield the thermochromic microcapsules and mitigate photodegradation. The primary objective was to evaluate the long-term performance and durability of the coatings in two contrasting Brazilian climates: Manaus, characterized by extreme heat and humidity, and Curitiba, which experiences seasonal temperature variations, based on a 2050 climate scenario. The coatings were applied to ceramic and fiber

cement roof tiles, and solar reflectance data from laboratory measurements were integrated into EnergyPlus simulations. These simulations assessed the energy impact of the coatings on a social housing model in both cities, exploring their potential to enhance energy efficiency and emphasizing the need for region-specific material solutions to optimize energy savings and thermal comfort.

2. Material and methods

2.1. Coating preparation and solar reflectance characterization

Two thermochromic coatings were developed: one with a protective TiO_2-P25 layer to prevent photodegradation, and the other without it. The composition of these coatings was defined by the mass ratio of the pigments to the colloidal silica solution base. The thermochromic (TC) layer was formulated by dispersing 7 % thermochromic pigment (ChromaZone, TMC Hallcrest, GB) together with 5 % fine rutile TiO_2 (Labsynth, BR) in an aqueous colloidal silica solution (Levasil FX-401, Nouryon AB, SE). The additional protective layer was created for long-term performance by incorporating 1 % TiO_2-P25 (Aeroxide TiO_2 P25, Evonik, DE) into the same aqueous colloidal silica solution.

This approach aimed to assess the impact of adding a TiO_2-P25 layer on the long-term performance of an organic thermochromic coating, using solar reflectance as a parameter to quantify degradation through accelerated aging. The coatings were applied with a foam roller to 70 × 20 × 5 mm ceramic and fiber cement roof tile samples, achieving average coverages of 144.3 g/m^2 and 175.0 g/m^2, respectively. The higher porosity of fiber cement led to greater absorption and material deposition compared to ceramic tiles, resulting in average layer thicknesses of 0.025 mm for ceramic and 0.031 mm for fiber cement. As this study focuses on energy consumption simulations, future research will explore the effects of both natural and accelerated aging on coating thicknesses in more detail.

In addition to the thermochromic samples, two baseline samples were prepared: one with uncoated tiles, serving as a reference, and another with conventional white acrylic paint (Matt Snow White, Suvinil, BR), used as a standard cool surface. Six samples of each paint-substrate combination were tested to determine average solar reflectance under lab conditions, minimizing random variation and improving result reliability. In total, 48 samples were measured (24 per substrate). More information on the design, characterization, and preparation of this coating can be found in a related publication by the same authors [37].

The thermochromic material's TT was determined by Differential Scanning Calorimetry (DSC), which detects phase changes through heat flow peaks during controlled heating and cooling. The cooling cycle yielded more consistent results, better reflecting real-world behavior. As detailed in a related publication [37], the second exothermic peak at 35.15 °C was selected as the TT due to its stability and repeatability. Unlike the first heating cycle, which can be influenced by processing history, this peak provides a more reliable indicator of the material's switching behavior.

The sample's solar reflectance (ρ) was measured using a spectrophotometer equipped with a diffuse reflectance accessory (DRA) with a 110 mm integrating sphere. This high-precision analysis scanned the entire solar spectrum, including its three main bands (UV, VIS, IR). It provided a detailed assessment of solar reflectance in the 300-2500 nm range, where most solar energy is concentrated. Measurements were performed using an Agilent CARY 5000 UV-VIS-NIR spectrophotometer (Fig. 1). They followed ASTM E903 [38], which describes a method for determining the solar optical properties of materials using integrating sphere spectrophotometry. The ASTM G173 [39] hemispherical solar irradiance spectrum, which provides standard terrestrial spectral data for sun-facing surfaces under reference atmospheric conditions, was used to adjust the measurements and ensure that they accurately reflect the material's behavior in real sunlight.

To evaluate the solar reflectance below the thermochromic transition temperature (TT) of 35 °C, as determined by DSC, the samples were first measured at room temperature (19 °C). Reflectance measurements above the TT were then performed by heating the samples to approximately 60 °C before measurement using a Corning 4 × 5 Inch Top PC-220 Hot Plate/Stirrer (120 V/60 Hz). At this stage, the samples remained in their colorless (high temperature) phase, and their surface temperatures were monitored using a K-type thermocouple connected to a Fluke 116 HVAC/R multimeter. The target temperature of 60 °C was chosen to ensure the samples remained at least 15 °C above the transition point throughout the solar reflectance measurement process. This safety margin was essential to maintain stable coloration in the high-temperature phase at all measured wavelengths.

2.2. Accelerated aging test

The accelerated aging procedure used in this study is based on ASTM D7897 [36], a laboratory standard developed to replicate the effects of three years of natural weathering on roofing materials in just a few days. It applies to various products, including coatings, membranes, shingles, tiles, and metals. The method simulates the typical degradation of solar reflectance and thermal emittance caused by dust accumulation, microbial growth, and changes in the material's surface due to sunlight, moisture, and heat. Although the standard was developed based on climatic conditions in North America, which may not reflect those in other regions, it remains the only existing protocol specifically tailored for accelerated aging of roofing systems and was therefore selected for this study.

The method was validated through the development of three contaminant mixtures designed to reproduce the aged optical characteristics of roofing materials exposed for three years in different climates: hot and humid (Miami, Florida), hot and dry (Phoenix, Arizona),

Fig. 1. a) Cary 5000 UV-VIS-NIR; b) TC+P25 samples above and below TT.

and polluted temperate (Cleveland, Ohio). A fourth mixture was created to represent the average aging effects observed in these locations and is used by the Cool Roof Rating Council (CRRC) to certify roofing products in the U.S. The process was tested on 25 products, including membranes, coatings, tiles, and shingles, and successfully replicated the CRRC's 3-year aged solar reflectance values [40].

The standard procedure consisted of three main steps. First, the samples were exposed to UV light in an accelerated weathering tester (Fig. 2) for 24 hours, divided into two cycles of 8 hours of UV radiation at 0.89 W/m^2/nm followed by 4 hours of condensation at 50 °C. Next, a calibrated aqueous contaminant mixture was applied using a pressurized tank. In this study, the fourth mixture, representing the average contaminant composition (47 % dust, 20 % salts, 28 % organic matter, and 5 % soot), was adopted as the test condition (Fig. 3). After this soiling phase, the samples underwent another 24-hour UV exposure under the same conditions as in the first step. Between each phase, they were dried under IR lamps. The weathering tester procedure was performed in a QUV chamber (Q-Lab), which simulated outdoor weathering by alternating UV radiation and humidity. This study evaluated only the samples' solar absorptance (α) before and after the aging test. This property was calculated from the measured solar reflectance (ρ), using the formula $\alpha = 1 - \rho$, according to ASTM G173 [39].

2.3. Simulations

2.3.1. Software selection

To accurately simulate the variable optical behavior of thermochromic pigments, it is essential to understand the commonly used methods and tools in this field. The adaptive behavior of these pigments requires specialized programming beyond conventional simulation techniques. To identify strategies for the simulation of thermochromic pigments applied to opaque materials in building envelopes, a Scopus search was conducted on 02 October 2024.

The aim was to provide a basis for the simulation process by highlighting existing practices and reliable software options. The following search terms were used: [(thermochromic) AND (energy OR (energy AND efficiency) OR (energy AND savings)) AND (roof OR wall OR facade OR envelope OR coating)]. The search was limited to English-language publications from 2018 onward, yielding 256 records. Of these, 23 studies specifically focused on the application of organic thermochromic pigments on roofs, aligning with the scope of this paper, and were selected to identify the main simulation methods and software used (Table 1). This focus helped minimize variability from other building envelope elements, enabling a more consistent and detailed comparison between studies and facilitating the identification of the most suitable tools for future research.

Amongst the 11 papers that detailed the methods used within the simulation software, 6 used the Energy Management System (EMS) in EnergyPlus to simulate the adaptive behavior of thermochromic materials. According to the EnergyPlus EMS Application Guide [56], EMS is an advanced feature that requires custom programming and a deep understanding of model behavior. It allows users to write small EMS programs to address specific questions and provides high-level control over various modeling aspects. For this study, SketchUp (version 2023) was chosen for modeling, with the Euclid (version 9.4.4) plug-in linking the 3D model to the EnergyPlus (version 24.2) simulation software. The EMS in EnergyPlus was used to simulate the behavior of the thermochromic coating, with the only parameter changed during the simulation being the solar absorptance (α) of the roof surface. This property was calculated from the measured solar reflectance (ρ) using the formula $\alpha = 1 - \rho$, according to ASTM G173 [39].

2.3.2. Location

To evaluate the impact of accelerated aging on the annual energy consumption of a social housing unit in Brazil, two climatically contrasting cities were selected: Manaus and Curitiba (Fig. 4). These cities represent the extremes of the Brazilian climate, offering valuable insights into thermochromic coatings' performance under different conditions. Manaus (Zone 0A [57], Zone 8 [58]) has a humid equatorial climate with consistently high temperatures and humidity, requiring large openings, passive cooling strategies, and reflective lightweight envelope to reduce heat gain. In contrast, Curitiba (Zone 3A [57], Zone 1 [58]) has a subtropical climate with significant seasonal variations, where winter strategies prioritize solar heat gain and thermal inertia, while summer strategies focus on shading and ventilation. The pronounced seasonal variations in Curitiba make it an ideal location for studying thermochromic coatings, which adjust their solar reflectance throughout the year in response to the surface temperature.

2.3.3. Building model

This study evaluates the impact of thermochromic coatings on the thermal performance of roof tiles using the *Minha Casa Minha Vida* (MCMV) model house as a reference. MCMV, a Brazilian government program for low-income housing [59], uses a nationwide standardized design, regardless of regional climatic conditions. This model represents a large part of the Brazilian housing stock, especially in peri-urban areas where MCMV houses are common, making it highly relevant in environmental and social contexts. Its widespread use in different climatic zones makes it a suitable reference for evaluating passive solutions, such as cool and thermochromic coatings, whose performance depends on local climatic conditions.

The building represents a 50 m^2 house with two bedrooms, one bathroom, and a combined kitchen and living room, with a pitched roof over an unventilated attic (Fig. 5). The simulations varied only the roof tile material and its solar absorptance based on the coating. The house includes standardized openings: doors (kitchen/living room/bedroom: 0.8 × 2.1 m, bathroom: 0.7 × 2.1 m) and windows (kitchen/living room: 1.2 × 1.0 × 1.1 m, bedroom: 1.0 × 1.0 × 1.1 m, bathroom: 0.6 × 0.6 × 1.5 m). The simulation model used in this study is based on a validated baseline developed by researchers who previously used it to create metamodels for assessing thermal discomfort in low-cost Brazilian housing across multiple climate zones [60]. Their study, which included Monte Carlo simulations and multivariate regression, achieved high predictive accuracy ($R^2 > 0.95$ in most cases), confirming the robustness of the baseline model. Building on this validated foundation ensures the reliability of the simulations presented here.

2.3.4. Simulation inputs

Tables 2 and 3 present the physical properties of the materials, including the initial and aged solar absorptance (α) for both color states, above and below the TT of the roof coatings, based on Brazilian standards [61,62] and solar reflectance measurements. Table 4 lists the simulation input data based on Brazilian standards [62]. The building geometry was modeled in SketchUp (v. 2023) and linked to EnergyPlus (v. 24.2) to define the thermal characteristics. The EMS tool in the IDF controlled the thermochromic coatings: above 35 °C, they became more reflective, and below, they became less reflective. Climate data for 2050 were obtained from EPW files from the building simulation climate data repository Climate One Building[1], which provides bias-corrected future weather files for Brazilian capitals. These files were generated using climate projections from the CORDEX project (RCP2.6 and RCP8.5), based on several global and regional climate models. The methodology used to generate the Typical Meteorological Years (TMYs) is described in detail in Bracht et al. [63].

[1] Available at: https://climate.onebuilding.org/.

Fig. 2. Weathering apparatus: a) sample holder and UV lamps; b) QUV machine.

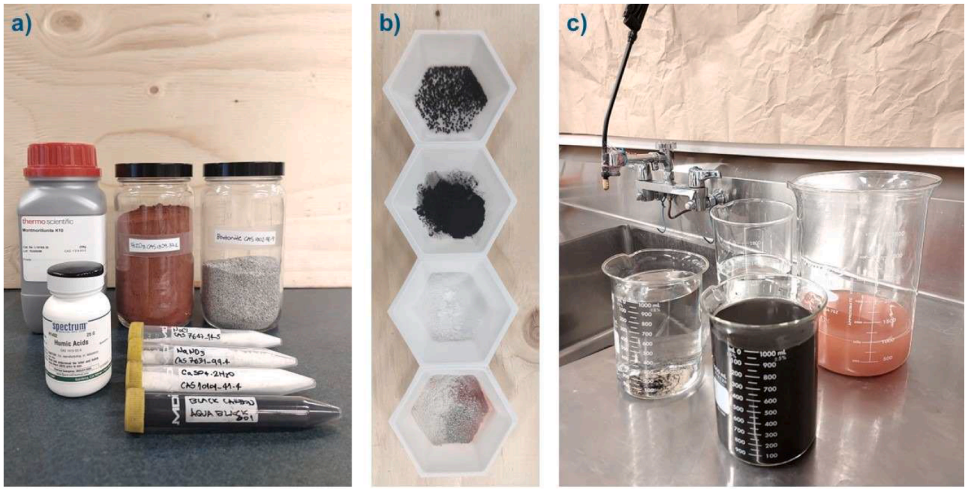

Fig. 3. Soiling material: a) reagents; b) soiling agents; c) soiling mixture and sprayer.

3. Results

3.1. Solar reflectance variation due to accelerated aging test

As explained in the methodology section, the effect of degradation on the samples was quantified using a single variable: solar absorptance, which was calculated based on the solar reflectance [39]. This was measured at two moments, before and after the accelerated aging test, and in both color states of the material, i.e., above and below the TT. As shown in Figs. 6 and 7, the solar reflectance of the reference samples, ceramic and fiber cement, remained stable after accelerated aging. Whether coated or not, ceramic substrates showed a consistent reflectance pattern, mainly in the shortwave IR range (1400-2500 nm). White samples showed a decrease in solar reflectance, especially in the VIS range (380-780 nm), as expected due to darkening from particulate deposition. However, they remained the most reflective of all the samples tested. The effect of accelerated aging on the solar reflectance of thermochromic coatings applied to both substrates was mainly observed as an approximation of the reflectance curves (indicated by the dashed lines in the graphs) for the two-color states (above and below the TT), particularly in the VIS range. This led to a noticeable loss of contrast between the light and dark states, especially in the TC samples.

Table 5 shows the effects of the accelerated aging test on the total solar absorptance (α) calculated from the laboratory-measured solar reflectance data ($\alpha = 1 - \rho$) [38]. The average variation between the initial and final solar absorptance values was 0.0145 for all samples, which agrees with the results of another study using the same method based on ASTM D7897 [36] for opaque building surfaces. In this study, carried out in Perugia, Italy, the mean variation was reported to be 0.01 [35].

The greatest change occurred in the white samples, consistent with the literature indicating that highly reflective (cool) surfaces degrade more due to particle deposition [64,65]. In contrast, reference samples of ceramic and fiber cement systems showed minimal changes in solar absorptance after accelerated aging. For the thermochromic samples, with or without the TiO_2-P25 layer, the average effect was 2.5 times greater in the uncolored state (above the TT) than in the colored state (below the TT). Solar absorptance decreased in the colored phase and increased in the uncolored phase, with the contrast between the two states decreasing, as showed in Figs. 6 and 7.

When averaging results across both ceramic and fiber cement substrates, the TC samples without the TiO_2-P25 layer showed significantly greater degradation in solar absorptance due to accelerated aging test. In the colored state (below TT), aging effects were about twice as severe compared to the TC+P25 samples; in the uncolored state (above TT), degradation was 1.5 times higher. In other words, the addition of the TiO_2-P25 layer reduced degradation by 50.4 % below TT and 33.3 % above TT. As shown in Fig. 8, despite its photocatalytic activity, TiO_2-

Table 1
Previous studies on thermochromic coatings for roofs have been conducted through simulation.

Reference	Year	Modeling	Simulation	Method
Kitsopoulou A. et al. [17]	2024	Design Builder	EnergyPlus	EMS (IDF)
Kitsopoulou A. et al. [41]	2024	Design Builder	Design Builder	CFD
Song G. et al. [42]	2024	Sketchup	EnergyPlus	-
Guo N. et al. [15]	2024	Sketchup	EnergyPlus	-
Azevedo C.C.M. et al. [16]	2024	Design Builder	EnergyPlus	-
Lingfan S. et al. [43]	2024	Design Builder	EnergyPlus	EMS (IDF)
Guo N. et al. [44]	2023	-	EnergyPlus	-
Vakilinezhad R.; Khabir S [45]	2023	Design Builder	EnergyPlus	-
Ji R.; Li X [46]	2023	-	EnergyPlus	EMS (IDF)
Kitsopoulou A. et al. [47]	2023	Design Builder	EnergyPlus	PCM
Sánchez E.C.; Vilà D. M [48]	2022	Design Builder	EnergyPlus	-
Cheng H. et al. [25]	2022	Sketchup	EnergyPlus	-
Zinzi M. et al. [49]	2021	TRNSYS	TRNSYS	Slow Hysteresis
Butt A.A. et al. [50]	2021	Sketchup	EnergyPlus	EMS (IDF)
Liu H.; Jiang T [23]	2021	Sketchup	EnergyPlus	-
Hu J.; Yu X [51]	2020	Sketchup	EnergyPlus	-
Berardi et al. [10]	2020	Honeybee	EnergyPlus	EMS (IDF)
Yuxuan Z. et al. [11]	2020	Sketchup	EnergyPlus	-
Granadeiro V. et al. [52]	2020	ESP-r	ESP-r	-
Fabiani C. et al. [53]	2020	-	-	CFD/FDM
Hu J.; Yu X [54]	2019	Sketchup	EnergyPlus	-
Hu J.; Yu X [6]	2019	Sketchup	EnergyPlus	EMS (IDF)
Fabiani C.; Pisello A. L [55]	2019	-	-	UCM

P25 did not harm the thermochromic dye. On the contrary, it helped preserve the pigment's color by slowing down photodegradation. This protective effect was more pronounced in areas with higher TiO_2-P25 content, likely due to its ability to absorb UV radiation and reinforce the microcapsule shell, reducing oxidation. These findings suggest that incorporating nano- TiO_2-P25 enhances the durability of thermochromic coatings by increasing their resistance to UV exposure and particle accumulation. Given that the stability of thermochromic pigments depends on sunlight intensity, temperature variation, and switching frequency, the protective action of TiO_2-P25 may help extend service life by neutralizing free radicals that drive degradation, something previous studies have shown can happen within days of natural exposure [20].

Fig. 8 shows the visual effect of accelerated aging test on samples coated with TC and TC+P25. The main degradation factor was UV radiation, rather than the deposition of the soiling mixture, which caused the thermochromic microcapsules to lose their original color. This is consistent with the solar reflectance curves (Figs. 6 and 7), where a decrease in color contrast was observed above and below TT. Initially, the TC (Fig. 8a) paint showed a more uniform and darker pigmentation than TC+P25 (Fig. 8b) because TiO_2-P25, a white powder, brightens the final coating. Although the paint containing TC+P25 appeared less uniform and mottled, its presence helped protect the coating from photodegradation. Areas with higher concentrations of TiO_2-P25, visible as lighter clusters, retained more of the original thermochromic color.

When the aged TC and TC+P25 (Fig. 8c) samples are compared, the protective effect of TiO_2-P25 becomes even more apparent. Although the initial TC coating was darker, TC+P25 retained a pigmentation closer to its original state after aging. This result confirms that the presence of TiO_2-P25 effectively slowed the photodegradation of thermochromic pigments and suggests that additives can help protect thermochromic materials when applied to opaque building surfaces.

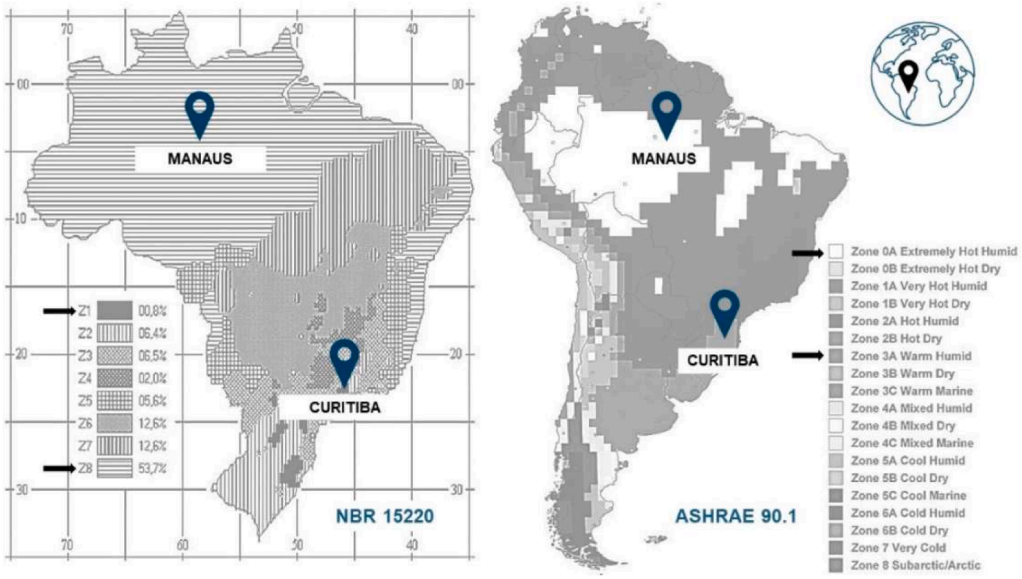

Fig. 4. a) Brazilian Bioclimatic Zones [58]; b) ASHRAE Bioclimatic Zones [57].

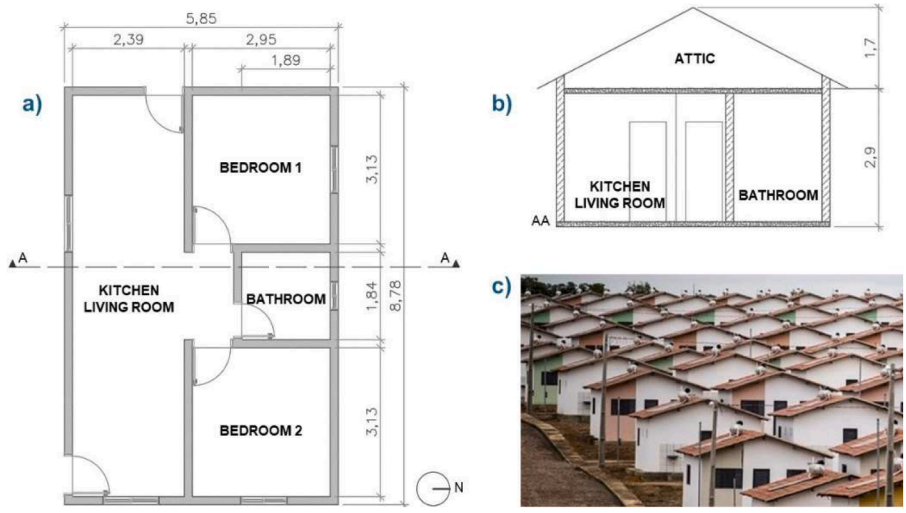

Fig. 5. a) Floor Plan; b) Cross-section; c) typical houses built in the MCMV program.

Table 2
Construction materials properties.

Inputs	t	λ	ρ	c	α
Concrete 10 cm	0.1	1.75	2200	1000	0.8
External / Internal mortar	0.025	1.15	2000	1000	0.6
Clay stretcher brick	0.02	0.9	1400	920	-
Slab mortar	0.005	1.15	2000	1000	-
Slab concrete	0.02	1.75	2200	1000	-
Slab clay	0.02	0.9	1400	920	-
Wood	0.035	0.29	700	1340	-

Legend: t: thickness (m); λ: thermal conductivity (W/m-K); ρ: density (Kg/m^3); c: specific heat capacity (J/Kg-K); α: solar absorptance.

Table 3
Roof properties.

Inputs	t	λ	ρ	c	α
Ceramic_Reference_initial	0.01	0.9	1400	920	0.476
Ceramic_Reference_aged	0.01	0.9	1400	920	0.505
Ceramic_White_initial	0.01	0.9	1400	920	0.118
Ceramic_White_aged	0.01	0.9	1400	920	0.172
Ceramic_TC _initial	0.01	0.9	1400	920	0.404 / 0.186
Ceramic_TC_aged	0.01	0.9	1400	920	0.314 / 0.267
Ceramic_TC+P25_initial	0.01	0.9	1400	920	0.371 / 0.183
Ceramic_TC+P25_aged	0.01	0.9	1400	920	0.329 / 0.258
Fiber cement_Reference_initial	0.004	0.65	1600	840	0.593
Fiber cement_Reference_aged	0.004	0.65	1600	840	0.590
Fiber cement_White_initial	0.004	0.65	1600	840	0.143
Fiber cement_White_aged	0.004	0.65	1600	840	0.200
Fiber cement_TC _initial	0.004	0.65	1600	840	0.433 / 0.209
Fiber cement_TC_aged	0.004	0.65	1600	840	0.358 / 0.297
Fiber cement_TC+P25_initial	0.004	0.65	1600	840	0.393 / 0.196
Fiber cement_TC+P25_aged	0.004	0.65	1600	840	0.360 / 0.244

Legend: t: thickness (m); λ: thermal conductivity (W/m-K); ρ: density (Kg/m^3); c: specific heat capacity (J/Kg-K); α: solar absorptance.

Table 4
Simulation inputs.

Input	Parameters
Site	North, according to Fig. 5a, Climates: Manaus/Curitiba (2050)
Materials	Table 1
Windows	6 mm clear glass; U-factor of 6.01 W/m^2-K; SHGC of 0.86
Construction	Walls: ceramic blocks with internal and external mortar coating; Floor: 10 cm solid concrete; Slab: concrete and ceramic with mortar coating; Roof: ceramic or fiber cement tiles with reference, white, and thermochromic finishes (new and aged).
Zones	5 simulation zones: Bedroom 1, Bedroom 2, Bathroom, Living Room, Kitchen, and Attic
People	People sleeping | Bedroom 1 and 2: 2 people from 22 h - 8 h People sitting | Living Room and Kitchen: 2 people from 14h-18h and 4 from 18h-22h;
Lighting	Bedroom: ON from 6 h – 8 h and 22 h – 0 h; Living Room and Kitchen: ON from 16 h -22 h;
Equipment	Living Room and Kitchen: ON from 14 h -22 h;
HVAC	Bedroom: ON 22 h - 8 h; Living Room and Kitchen: ON 14 h – 22 h. Both when Tar>25 °C and Tar<18 °C.
EMS	Sensor: Object: Gable Roof (Building Surface); Variable: Surface Outside Face Temperature Actuator: Object: Roof Tile (Material); Component control type: Surface Property Solar Absorptance Program Calling Manager: Calling Point: AfterPredictorBeforeHVACManagers Program (example for sample TC+P25 aged): Name: AdjustMaterialProperties; Conditions: If WarmupFlag == 0 and 1 ≤ DayOfYear ≤ 365 and RoofSurfaceTempA ≥ 35, then RoofSolarAbsorptanceActuator = 0.258; If WarmupFlag == 0 and 1 ≤ DayOfYear ≤ 365 and RoofSurfaceTempA < 35, then RoofSolarAbsorptanceActuator = 0.329; If WarmupFlag == 0 and 1 ≤ DayOfYear ≤ 365 and RoofSurfaceTempB ≥ 35, then RoofSolarAbsorptanceActuator = 0.258; If WarmupFlag == 0 and 1 ≤ DayOfYear ≤ 365 and RoofSurfaceTempB < 35, then RoofSolarAbsorptanceActuator = 0.329

3.2. Impact on energy consumption

Fig. 9 compares the energy needs of the two cities. Manaus, with a hot and humid climate, only requires cooling (CLG) to alleviate heat discomfort. In contrast, with a subtropical, milder and more variable environment, Curitiba requires heating (HTG) and cooling (CLG). However, Curitiba's total energy demand is only 20 % of Manaus's, as its climate naturally balances heating and cooling needs.

Table 6 shows that the white (cool) coatings had the lowest annual energy loads, both before and after aging. In Manaus, as expected, they were the most effective passive cooling strategy, since highly reflective surfaces are ideal for hot climates. In Curitiba, however, these same coatings led to higher heating loads due to the "winter penalty," where high solar reflectance reduced solar heat gain during colder months. Even with this drawback, white coatings still had the best overall energy performance in Curitiba throughout the year. This was somewhat unexpected, as thermochromic pigments are designed to adapt to seasonal variations by reducing cooling needs in summer and allowing more heat gain in winter. Ideally, they would offer a better year-round energy balance. However, the thermochromic pigment tested in this study did

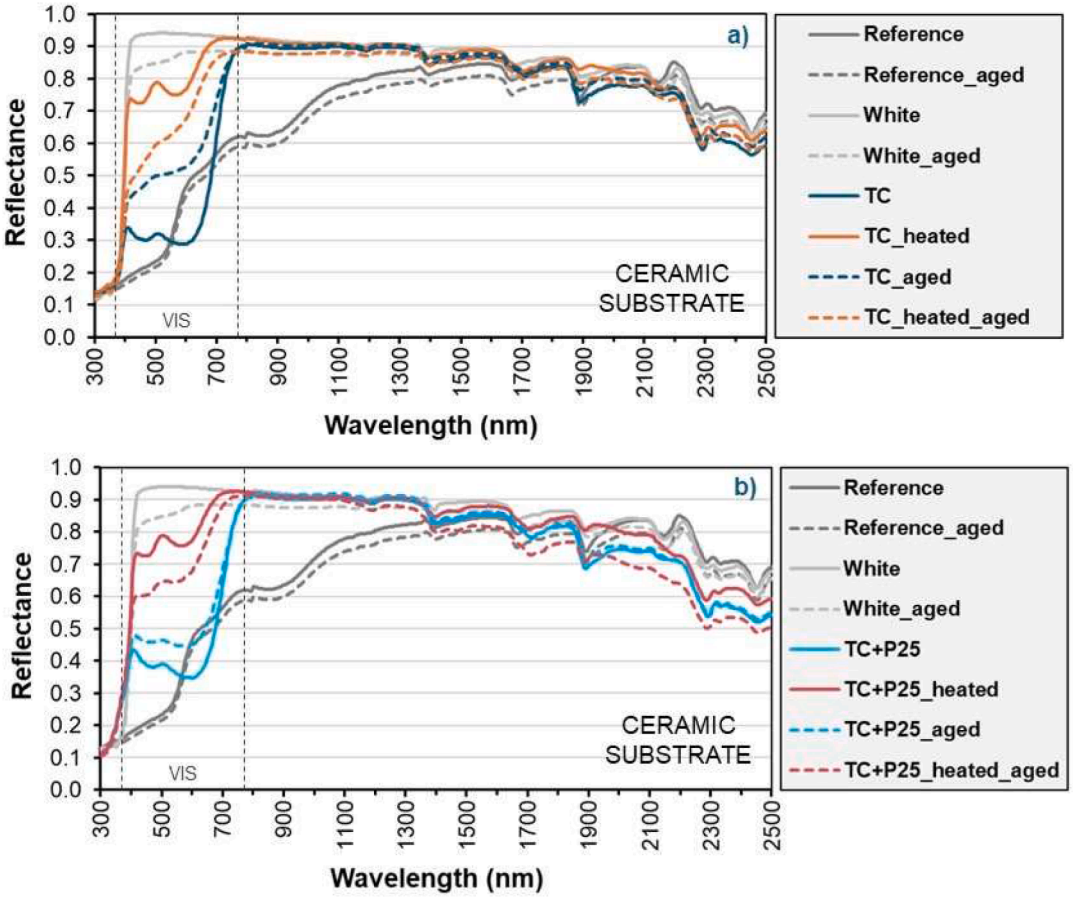

Fig. 6. Solar reflectance curves (UV-VIS-IR) of ceramic samples: a) TC; b) TC+P25.
Legend: Aged: after accelerated aging test; Heated: above TT.

not outperform the white coating.

It is important to note that these results are closely tied to the characteristics of the MCMV house model used in the simulations. As a standardized and widely implemented housing typology in Brazil, it highlights the need to tailor passive strategies to specific climatic conditions. In a country with such diverse climates, uniform solutions often fall short. Still, the model's widespread use makes the findings relevant to real-world applications, especially in the context of social housing.

Table 7 shows the effect of solar absorptance degradation on energy demand. White samples showed the greatest variation, consistent with their significant loss of solar absorptance due to weathering. Although thermochromic samples (TC and TC+P25) also showed significant degradation in solar absorptance, their annual energy demand remained stable. This suggests that accelerated weathering affects absorptance values more than the overall energy performance of the building. A comparison of the percentage variation in the aging impact on solar absorptance, presented in Table 5, reveals that the percentage variations in Table 7 are significantly smaller.

3.3. Investigation of an ideal thermochromic material

Among the samples developed in this study, the white samples showed the lowest annual energy consumption in Curitiba, both before and after aging, which was unexpected. A study was carried out to identify the ideal thermochromic material for this specific climate using only the ceramic roof substrate as a base material. Ten scenarios were considered: (1-2) ceramic reference samples, which served as a performance baseline in both their non-aged and aged states; (3-4) white samples, which served as a performance baseline in both their non-aged and aged states; (5) a hypothetical ideal thermochromic pigment with significantly different solar absorptance values above and below the transition temperature (TT), ensuring a marked distinction between color phases; (6) pure powder thermochromic pigment, using real solar absorptance data measured in the laboratory; (7-10) the thermochromic coatings developed in this study (TC and TC+P25), both before and after aging. The TT was also varied in this study to evaluate an ideal case.

Fig. 10 shows that using a high contrast thermochromic pigment with the same TT as the original coating (35 °C) did not reduce the energy demand for the HVAC system in the Curitiba climate. However, if the TT is lowered while the color contrast of this ideal thermochromic pigment remains the same, the energy consumption decreases significantly. The lowest energy demand was observed at a TT of 20 °C, suggesting that this is the optimal switching temperature for minimizing HVAC loads under Curitiba's specific climatic conditions.

Before aging, the TC and TC+P25 coatings performed similarly, with almost identical energy consumption demand curves. However, after accelerated aging, the TiO_2-P25 protective layer proved effective in preserving the surface properties of the coating, reducing degradation, and lowering energy consumption compared to the unprotected TC sample. At a TT of 20 °C, the aged TC+P25 coating outperformed the aged TC and matched the performance of the aged white sample. This is consistent with the results in Section 3.1, which showed that the TiO_2-P25 layer helped reduce color degradation. As a result, the thermochromic behavior, specifically the ability to change color between states, was better maintained, preserving contrast and functionality.

Using the uncoated ceramic reference substrate as a baseline, the simulations showed that the ideal high-contrast thermochromic pigment with a TT of 20 °C could reduce annual thermal energy demand by 11.3

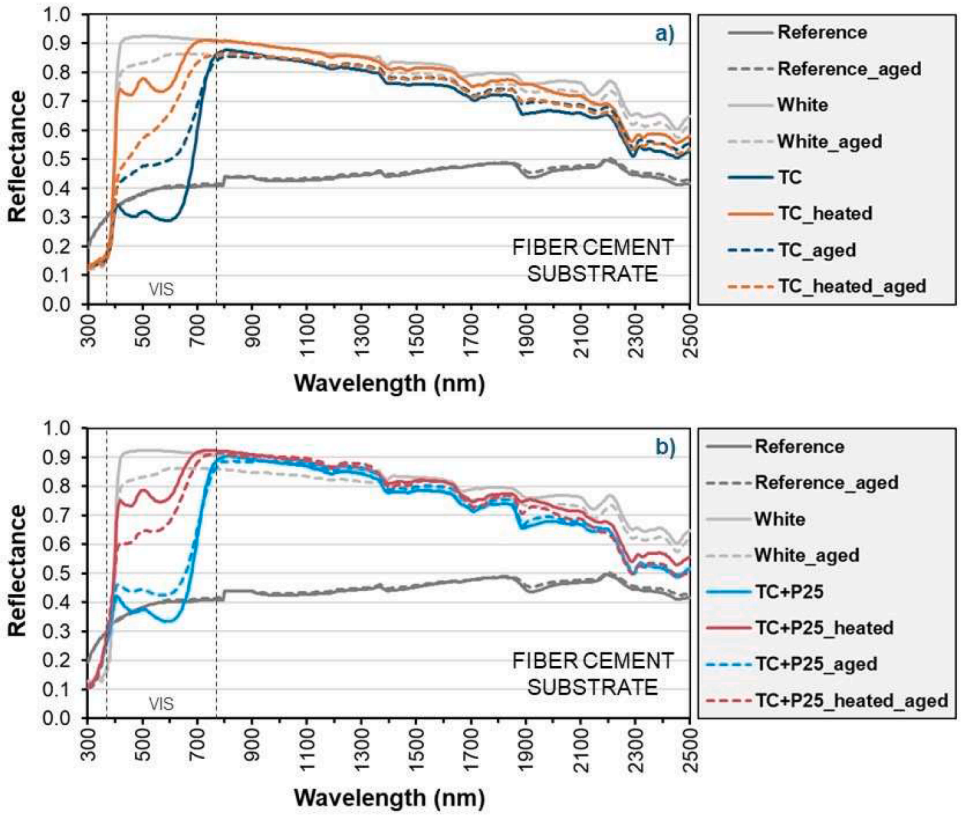

Fig. 7. Solar reflectance curves (UV-VIS-IR) of fiber cement samples: a) TC; b) TC+P25.
Legend: Aged: after accelerated aging test; Heated: above TT.

Table 5
Effect of aging on solar absorptance (α).

Samples	Initial α	Initial α (heated)	Aged α	Aged α (heated)	α Δ %	α Δ % (heated)
Ceramic_Reference	0.476	-	0.505	-	6.1 %	-
Fiber cement_Reference	0.593	-	0.590	-	-0.5 %	-
Ceramic_White	0.118	-	0.172	-	45.8 %	-
Fiber cement_White	0.143	-	0.200	-	39.9 %	-
Ceramic_TC	0.404	0.186	0.314	0.267	-22.3 %	43.5 %
Fiber cement_TC	0.433	0.209	0.358	0.297	-17.3 %	42.1 %
Ceramic_TC+P25	0.371	0.183	0.329	0.243	-11.3 %	32.8 %
Fiber cement_TC+P25	0.393	0.196	0.360	0.244	-8.4 %	24.5 %

Legend: Initial: non-aged; Aged: after accelerated aging test; Heated: above TT.

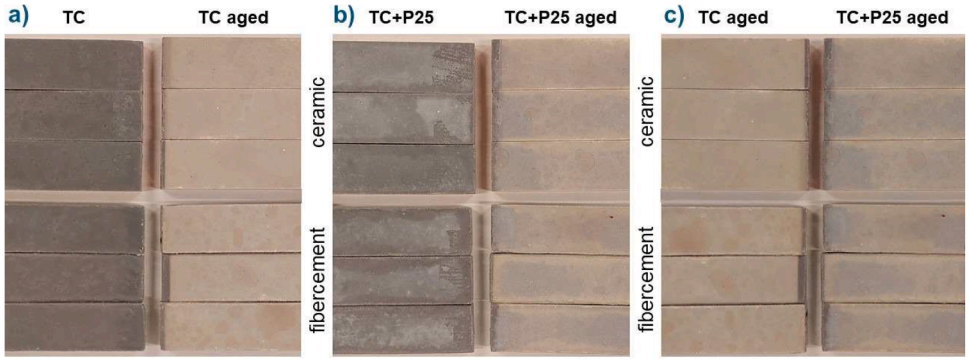

Fig. 8. Aging effect, on room temperature: a) TC samples, b) TC+P25, c) TC x TC+P25.
Legend: Aged: after accelerated aging test.

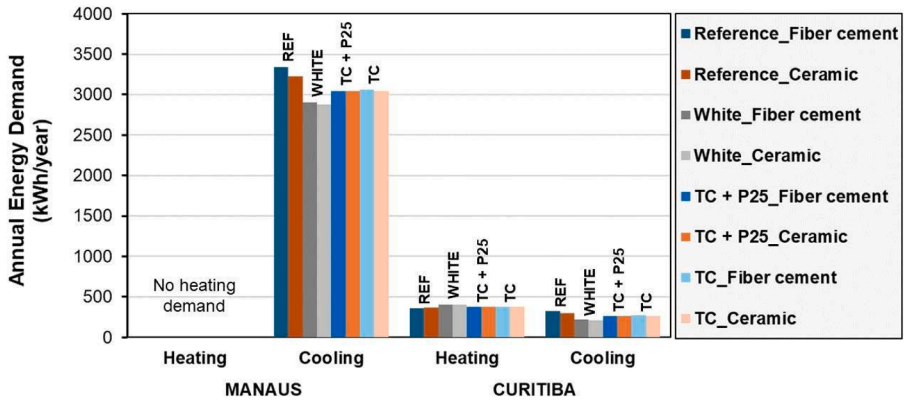

Fig. 9. Initial annual energy demand (non-aged samples).

Table 6
Effect of aging on annual cooling and heating loads (kWh/year).

Samples	Initial Manaus (CLG)	Aged Manaus (CLG)	Initial Curitiba (HTG)	Aged Curitiba (HTG)	Initial Curitiba (CLG)	Aged Curitiba (CLG)
Ceramic_Reference	3225	3252	366	364	297	304
Fiber cement_Reference	3335	3333	357	357	327	327
Ceramic_White	2882	2934	405	399	213	225
Fiber cement_White	2903	2958	404	397	219	232
Ceramic_TC	3046	3046	374	383	266	255
Fiber cement_TC	3061	3075	373	380	271	264
Ceramic_TC+P25	3047	3040	377	381	261	257
Fiber cement_TC+P25	3045	3050	377	380	265	262

Legend: Initial: non-aged; Aged: after accelerated aging test; CLG: Cooling Load; HTG: Heating Load.

Table 7
Percentage variation in total annual energy demand due to accelerated aging (kWh/year).

Samples	Initial Manaus	Initial Curitiba	Aged Manaus	Aged Curitiba	Δ % Manaus	Δ % Curitiba
Ceramic_Reference	3225	663	3252	667	0.86 %	0.65 %
Fibercement_Reference	3335	684	3333	684	-0.09 %	-0.07 %
Ceramic_White	2882	618	2934	624	1.81 %	0.96 %
Fiber cement_White	2903	622	2958	629	1.90 %	1.04 %
Ceramic_TC	3046	640	3046	638	-0.03 %	-0.26 %
Fiber cement_TC	3061	644	3075	644	0.45 %	0.09 %
Ceramic_TC+P25	3047	639	3040	638	-0.22 %	-0.08 %
Fiber cement_TC+P25	3045	642	3050	642	0.17 %	-0.02 %

Legend: Initial: non-aged; Aged: after accelerated aging test.

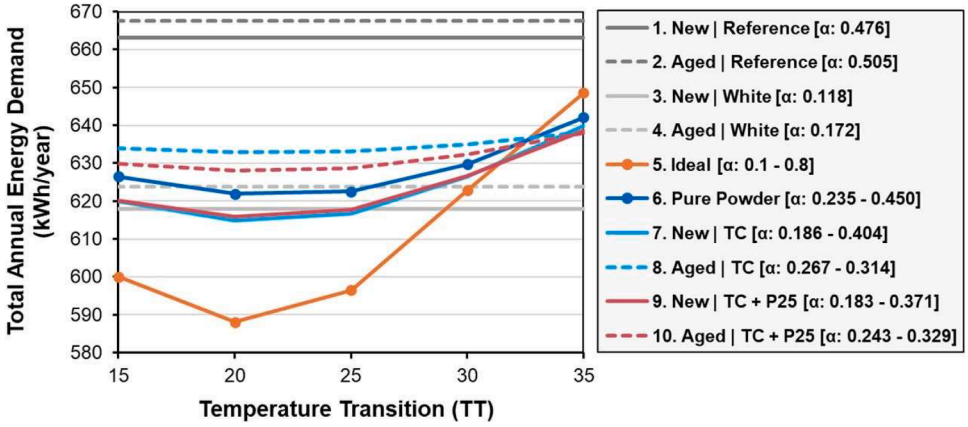

Fig. 10. Ideal thermochromic material investigation for Curitiba's climate.

%. Among the thermochromic coatings analyzed, the unaged TC sample reduced energy consumption by 7.3 %, while the aged one achieved a 5.2 % reduction. The TC+P25 coating showed similar results, with reductions of 7.1 % when new and 5.9 % after aging.

However, as shown in the graph (Fig. 10), the thermochromic coatings only outperformed the white coating when the TT was lowered to 20 °C, and even then, the energy savings were modest: only 0.34 % for TC+P25 and 0.48 % for TC compared to the white reference. After aging, the white sample consistently outperformed both thermochromic coatings. This shows that it is not enough to match the TT to the local climate simply; a strong contrast between the two-color states of the pigment is also essential, as shown by the simulated performance of the hypothetical ideal pigment.

When examining the energy variation as a function of TT, the TC and TC+P25 coatings showed reductions of 3.9 % and 3.6 %, respectively, when comparing their energy demand at 35 °C (baseline) and 20 °C (optimized). This confirms the effectiveness of the TT adjustment in reducing the energy demand when the pigment composition remains constant. For the aged samples, the effect was smaller: 0.8 % for TC and 1.6 % for TC+P25. The improvement observed in the TC+P25 samples was twice as high as in the TC samples, further reinforcing the protective role of the TiO_2-P25 layer in reducing the impact of aging.

4. Discussion

A comparison between the energy demands of two Brazilian cities with contrasting climates underscores the importance of adapting passive strategies to local conditions. The results show that standardized solutions are often ineffective in a country as climatically diverse as Brazil. Designing buildings that respond to regional thermal demands is crucial not only to reduce reliance on artificial cooling and heating, but also to lower energy costs, mitigate greenhouse gas emissions and promote more energy-efficient and comfortable buildings.

As discussed throughout this work, there is a clear need to develop and update accelerated aging standards, particularly those tailored to local conditions. In the absence of a Brazilian standard that addresses this issue, this study adopted a widely recognized international guideline published by ASTM (American Society for Testing and Materials), based on research conducted in the United States. Although this choice offers a solid methodological foundation, it also presents limitations, especially regarding climatic differences and the chemical and physical characteristics of particulate matter deposited on surfaces, which may vary significantly under Brazilian conditions and affect the degradation behavior of the coatings.

Simulation results for the thermochromic coating showed that lowering the TT from 35 °C to 20 °C significantly increased energy savings in the Curitiba climate, especially for unaged samples. Adjusting the TT to match local climatic conditions is a simple yet effective strategy to improve the performance of thermochromic coatings and should be considered in future developments. This adjustment is also feasible due to the wide availability of thermochromic materials with different TTs on the market. However, these benefits diminish after accelerated aging, highlighting the need to improve the durability of these materials.

Another promising direction for future research is to increase the optical contrast between the colored and uncolored phases of the pigment, which would improve the effectiveness of the coating in both heating and cooling modes. However, achieving this is more complex as it requires chemical modifications to the pigment and a deeper understanding of its interaction with other coating components and its resistance to photodegradation.

Compared to other studies, the decrease in energy consumption observed here are in a similar range. Overall, the literature reviewed in this paper reports a reduction in energy demand of 2 % to 17 % across different climates [9–17]. Although our analysis focused on small samples, the decrease of about 5-7 % is in line with these findings, highlighting the potential of thermochromic coatings for improving energy efficiency. Furthermore, by increasing the contrast and adjusting the TT to local conditions, energy savings could reach 11.33 % annually.

Regarding durability, our use of a TiO_2-P25-based protective layer is consistent with recent advances in smart coatings. Liu et al. [24] showed that UV-resistant coatings reduce reflectance losses due to dust and UV exposure, while Hussain et al. [29] demonstrated the protective role of SiO_2 encapsulation in thermochromic microcapsules. In this paper, the results shows that TC+P25 samples degraded 50.4 % less below the TT and 33.3 % less above the TT compared to TC samples, confirming that the TiO_2-P25 layer effectively mitigates photodegradation by enhancing resistance to UV radiation and particle accumulation. However, because TiO_2-P25 is a white powder before dispersion in the SiO_2 matrix, its addition tends to reduce the initial color contrast of the thermochromic coating. To address this limitation, future research should explore alternative encapsulation techniques or nanostructured protective layers that preserve optical contrast while improving durability. Overall, the enhanced stability and color retention observed in TC+P25 samples suggest that combining thermochromic pigments with protective coatings is a promising strategy for developing long-lasting, multifunctional surfaces.

5. Conclusions

This study evaluated the performance and durability of a dye-based thermochromic coating applied to ceramic and fiber cement tiles, with and without adding a TiO_2-P25 protective layer, under accelerated aging conditions. Solar absorptance, calculated from laboratory-measured solar reflectance, was the only variable input used in EnergyPlus simulations to compare the thermal impact of different surface conditions in two Brazilian cities with contrasting climates: Manaus and Curitiba.

The simulation results showed that lowering the pigment TT from 35 °C to 20 °C led to a 5–7 % reduction in annual energy demand in Curitiba, compared to the ceramic reference substrate, in both new and aged conditions. By optimizing both TT and optical contrast, savings could potentially reach 11.3 %. Although none of the coatings developed in this study outperformed conventional white paint regarding annual energy savings, the thermochromic pigments showed clear adaptive potential, especially in climates like Curitiba that require heating and cooling. With further optimization of TT and color contrast, these coatings could outperform white paint in such mixed climates. These results are consistent with previous studies that reported 2 % to 17 % of energy savings, depending on building and climate characteristics.

Durability analysis showed that adding a TiO_2-P25 protective layer significantly delayed pigment degradation. Under accelerated aging, the TC+P25 samples degraded about twice as slowly as the unprotected samples below the transition temperature and a third slower above the transition temperature, suggesting improved resistance to particle deposition and UV exposure. However, the addition of TiO_2-P25, which is a white pigment, slightly reduced the initial color contrast, a critical factor in adaptive performance. This highlights the need for improved formulations that maintain contrast while enhancing resistance to photodegradation.

Overall, the results support the development of climate-responsive, energy-efficient coatings, especially in diverse climates such as Brazil. The results also highlight the need for updated, locally adapted accelerated aging standards, as current international methods may not fully represent Brazilian environmental conditions. Future studies should investigate nanoscale pigment modifications to enhance color contrast, explore alternative encapsulation techniques, and conduct natural weathering tests to optimize energy efficiency and long-term durability.

CRediT authorship contribution statement

Ana Carolina Hidalgo-Araujo: Writing – original draft, Methodology, Investigation, Formal analysis, Data curation. **Rafael Salomão:**

Methodology, Investigation, Formal analysis. **Umberto Berardi:** Writing – original draft, Supervision, Funding acquisition. **Kelen Almeida Dornelles:** Project administration, Methodology, Funding acquisition, Formal analysis.

Declaration of competing interest

The authors declare that they have no known competing financial interests or personal relationships that could have appeared to influence the work reported in this paper.

Acknowledgements

The authors thank the São Paulo Research Foundation FAPESP (Grants 2022/14074-5, 2022/03655-7, 2024/00850-9 and 2024/10060-5), HERA (Holistic Energy Recovery Agent tool for sustainable urban clusters, PRIN 2022) and NETPLUS (Neighborhood Energy Transition: towards Positive energy balance and carbon neutral districts, PRIN PNRR) for supporting this work. They also thank Nouryon Latin America (Brazil) and AB (Sweden) for supplying SiO_2.

Data availability

Data will be made available on request.

References

[1] IPCC, Climate Change 2022: Impacts, Adaptation and Vulnerability: Sixth Assessment Report of the Intergovernmental Panel on Climate Change, 2022. Intergovernmental Panel on Climate Change.
[2] A. Hakami, S.S. Srinivasan, P.K. Biswas, Review on thermochromic materials: development, characterization, and applications, J. Coat. Technol. Res. 19 (2022) 377–402, https://doi.org/10.1007/s11998-021-00558-x.
[3] M. Santamouris, G.Y. Yun, Recent development and research priorities on cool and super cool materials to mitigate urban heat island, Renew. Energy 161 (2020) 792–807, https://doi.org/10.1016/j.renene.2020.07.109.
[4] S. Garshasbi, M. Santamouris, Using advanced thermochromic technologies in the built environment: recent development and potential to decrease energy consumption and fight urban overheating, Solar Energy Mater. Solar Cells 191 (2019) 21–32, https://doi.org/10.1016/j.solmat.2018.10.023.
[5] C. Fabiani, A.L. Pisello, Passive cooling by means of adaptive cool materials, in: A. L. Pisello, F. Pacheco-Torgal, L. Czarnecki, L.F. Cabeza, & C.-G. Granqvist (Eds.), Eco-Efficient Materials for Reducing Cooling Needs in Buildings and Construction, Woodhead Publishing, 2021, pp. 439–457, https://doi.org/10.1016/B978-0-12-820791-8.00018-3.
[6] J. Hu, X.B. Yu, Adaptive thermochromic roof system: assessment of performance under different climates, Energy Build. 192 (2019) 1–14, https://doi.org/10.1016/j.enbuild.2019.02.040.
[7] T. Karlessi, M. Santamouris, K. Apostolakis, A. Synnefa, I. Livada, Development and testing of thermochromic coatings for buildings and urban structures, Solar Energy 83 (2009) 538–551, https://doi.org/10.1016/j.solener.2008.10.005.
[8] M. Santamouris, M. Santamouris, Chapter 8 - Mitigating the local climatic change and fighting urban vulnerability, Minimizing Energy Consumption, Energy Poverty and Global and Local Climate Change in the Built Environment: Innovating to Zero (2019) 223–307, https://doi.org/10.1016/B978-0-12-811417-9.00008-8.
[9] S. Soudian, U. Berardi, N. Laschuk, Development and thermal-optical characterization of a cementitious plaster with phase change materials and thermochromic paint, Solar Energy 205 (2020) 282–291, https://doi.org/10.1016/j.solener.2020.05.015.
[10] U. Berardi, M. Garai, T. Morselli, Preparation and assessment of the potential energy savings of thermochromic and cool coatings considering inter-building effects, Solar Energy 209 (2020) 493–504, https://doi.org/10.1016/j.solener.2020.09.015.
[11] Z. Yuxuan, Z. Yunyun, Y. Jianrong, Z. Xiaoqiang, Energy saving performance of thermochromic coatings with different colors for buildings, Energy Build. 215 (2020) 1–11, https://doi.org/10.1016/j.enbuild.2020.109920.
[12] E.C. Sánchez, D.M. Vilà, Thermochromic materials as passive roof technology: their impact on building energy performance, Energies 15 (6) (2022) 2161, https://doi.org/10.3390/en15062161.
[13] K. Khaled, U. Berardi, Z. Liao, Energy modelling and saving potential of polymeric solar-responsive thermochromic window films, Solar Energy 244 (2022) 84–103, https://doi.org/10.1016/j.solener.2022.08.008.
[14] G. Song, K. Zhang, F. Xiao, Z. Zhang, S. Jiao, Y. Gong, Building energy efficiency enhancement through thermo-chromic powder-based temperature-adaptive radiative cooling roofs, Buildings 14 (6) (2024) 1745, https://doi.org/10.3390/buildings14061745.
[15] N. Guo, S. Liu, C. Chen, S. Song, H. Mo, M. Yan, M. Chen, Outdoor adaptive temperature control based on a thermo-chromic hydrogel by regulating solar heating, Solar Energy (2024) 270, https://doi.org/10.1016/j.solener.2024.112405.
[16] C.C. de Azevedo, D.N. Amorim, M. Santamouris, Use of passive cooling techniques and super cool materials to minimize cooling energy and improve thermal comfort in Brazilian schools, Energy Build. (2024) 312, https://doi.org/10.1016/j.enbuild.2024.114125.
[17] A. Kitsopoulou, E. Bellos, C. Sammoutos, P. Lykas, M.G. Vrachopou-los, C. Tzivanidis, A detailed investigation of thermochromic dye-based roof coatings for Greek climatic conditions, J. Build. Eng. 84 (2024) 108570, https://doi.org/10.1016/j.jobe.2024.108570.
[18] Y. Ma, B. Zhu, K. Wu, Preparation of reversible thermochromic building coatings and their properties, J. Coat. Technol. 72 (927) (2000) 67–71, https://doi.org/10.1007/BF02720527.
[19] M. Sharma, M. Whaley, J. Chamberlain, T. Oswald, R. Schroden, A. Graham, M. Barger, B. Richey, Evaluation of thermochromic elastomeric roof coatings for low-slope roofs, Energy Build. 155 (2017) 459–466, https://doi.org/10.1016/j.enbuild.2017.09.030.
[20] E. Badino, G. Autretto, S. Fantucci, V. Serra, M. Zinzi, Development of testing procedures for assessing the thermal and optical performance of thermochromic coatings for buildings, Solar Energy 263 (2023) 111950, https://doi.org/10.1016/j.solener.2023.111950.
[21] Y. Xi, S. Xu, J. Zhang, Reversible thermochromic composites for intelligent adjustment of solar reflectance, Mater. Chem. Phys. 276 (2022) 125372, https://doi.org/10.1016/j.matchemphys.2021.125372.
[22] X. Sun, Y. Wu, S. Tang, Self-adaptive smart thermochromic film with quick response for all-year radiative cooling and solar heating, ACS Appl. Mater. Interfaces. 16 (49) (2024) 68407–68415, https://doi.org/10.1021/acsami.4c16273.
[23] S. Soudian, U. Berardi, N. Laschuk, Effects of long-term UV exposure on the performance of cement plasters integrated with thermochromic paint and PCMs for building facade applications, in: C. Serrat, J.R. Casas, V. Gibert (Eds.), Current Topics and Trends on Durability of Building Materials and Components, 2020. Retrieved from, https://www.scipedia.com/public/Soudian_et_al_2020a.
[24] H. Liu, T. Jiang, F. Wang, J. Ou, W. Li, Thermochromic superhydrophobic coatings for building energy conservation, Energy Build. 251 (2021) 111374, https://doi.org/10.1016/j.enbuild.2021.111374.
[25] S.R. Dantas, F. Vittorino, Comparison of reflectance to solar radiation between mortars treated with TiO2 and painted mortars after three years of exposure, J. Build. Eng. (2022) 46, https://doi.org/10.1016/j.jobe.2021.103829.
[26] K. Wang, M. Janczarek, Z. Wei, T. Raja-Mogan, M. Endo-Kimura, T.M. Khedr, B. Ohtani, E. Kowalska, Morphology- and crystalline composition-governed activity of titania-based photocatalysts: overview and perspective, Catalysts 9 (2019) 1054.
[27] X. Guo, L. Rao, P. Wang, C. Wang, T. Ao, W. Jiang, Y. Wang, Photocatalytic properties of P25-doped TiO2 composite film synthesized via sol-gel method on cement substrate, J. Environ. Sci. 66 (2018) 71–80, https://doi.org/10.1016/j.jes.2017.05.029.
[28] J. Hu, X.B. Yu, Design and characterization of energy efficient roofing system with innovative TiO2 enhanced thermo-chromic films, Constr. Build. Mater. 223 (2019) 1053–1062, https://doi.org/10.1016/j.conbuildmat.2019.06.003.
[29] M. Hussain, A.M. Sikandar, S. Nasir, W. Ahmed, Effect of SiO2 coated leuco-dye based thermochromic pigment on the properties of Portland cement pastes, J. Build. Eng. (2021) 35, https://doi.org/10.1016/j.jobe.2020.102019.
[30] H. Cheng, F. Wang, H. Liu, J. Ou, W. Li, R. Xue, Fabrication and properties of thermochromic superhydrophobic coatings, Adv. Eng. Mater. 24 (2022) 2100647, https://doi.org/10.1002/adem.202100647.
[31] Y. Li, Z. Jiang, F. He, X. Chen, P. Li, G. Wang, X. He, W. Zhu, Reversible thermochromic microcapsules with SiO2 shell for indicating temperature and thermoregulation, J. Energy Storage 72(D) (2023), https://doi.org/10.1016/j.est.2023.108674.
[32] A.C. Hidalgo-Araujo, R. Salomão, U. Berardi, K.A. Dornelles, Thermochromic materials for building applications: overview through a bibliometric analysis, Solar Energy 293 (2025) 113491, https://doi.org/10.1016/j.solener.2025.113491.
[33] U. Berardi, R.H. Nosrati, Long-term thermal conductivity of aerogel-enhanced insulating materials under different laboratory aging conditions, Energy 147 (2018) 1188–1202, https://doi.org/10.1016/j.energy.2018.01.053.
[34] U. Berardi, The impact of aging and environmental conditions on the effective thermal conductivity of several foam materials, Energy 182 (2019) 777–794, https://doi.org/10.1016/j.energy.2019.06.022.
[35] L.S.B. Couto, Evaluation of the Combined Effect of Different Climatic Conditions on the Natural Aging of Paints on Building Facades, Institute of Architecture and Urbanism, University of São Paulo, São Carlos, 2024. PhD Dissertation.
[36] ASTM, ASTM D7897-18 (Reapproved 2023) - Standard Practice for Laboratory Soiling and Weathering of Roofing Materials to Simulate Effects of Natural Exposure on Solar Reflectance and Thermal Emittance, American Society for Testing and Materials, 2023.
[37] A.C. Hidalgo-Araujo, R. Salomão, U. Berardi, K.A. Dornelles, Design and characterization of a SiO2-TiO2 coating containing organic and inorganic thermochromic pigments and optimized with TiO2-P25 for improved long-term performance in energy-efficient roofing, Solar Energy Mater. Solar Cells 289 (2025) 113655, https://doi.org/10.1016/j.solmat.2025.113655.
[38] ASTM, ASTM E903–20 - Standard Test Method for Solar Absorptance, Reflectance and Transmittance of Materials Using Integrating Spheres, American Society for Testing and Materials, 2020.

[39] ASTM, ASTM G173–23 - Standard Tables for Reference Solar Spectral Irradiances: Direct Normal and Hemispherical on 37° Tilted Surface, American Society for Testing and Materials, 2023.
[40] M. Sleiman, T.W. Kirchstetter, P. Berdahl, H.E. Gilbert, S. Quelen, L. Marlot, C. V. Preble, S. Chen, A. Montalbano, O. Rosseler, H. Akbari, R. Levinson, H. Destaillats, Soiling of building envelope surfaces and its effect on solar reflectance – Part II: Development of an accelerated aging method for roofing materials, Solar Energy Mater. Solar Cells 122 (2014) 271–281, https://doi.org/10.1016/j.solmat.2013.11.028.
[41] A. Kitsopoulou, D. Pallantzas, C. Sammoutos, P. Lykas, M. Bellos, G. Vrachopoulos, A. Tzivanidis, A comparative investigation of building rooftop retrofit actions using an energy and computer fluid dynamics approach, Energy Build. 315 (2024) 114326, https://doi.org/10.1016/j.enbuild.2024.114326.
[42] G. Song, K. Zhang, F. Xiao, Z. Zhang, S. Jiao, Y. Gong, Building energy efficiency enhancement through thermo-chromic powder-based temperature-adaptive radiative cooling roofs, Buildings 14 (6) (2024) 1745, https://doi.org/10.3390/buildings14061745.
[43] S. Lingfan, G. Lin, C. Hongbo, Improved energy-saving performance of a small office building using coupled phase change materials and thermochromic (PCM/TC) roof system, J. Energy Storage 100 (Part B) (2024), https://doi.org/10.1016/j.est.2024.113561.
[44] N. Guo, R. Yang, M. Chen, H. Yan, W. Chen, Self-adaptive colored radiative cooling by tuning visible spectra, Sol. RRL. 7 (2023) 2300512, https://doi.org/10.1002/solr.202300512.
[45] R. Vakilinezhad, S. Khabir, Evaluation of thermal and energy performance of cool envelopes on low-rise residential buildings in hot climates, J. Build. Eng. 72 (2023), https://doi.org/10.1016/j.jobe.2023.106643.
[46] R. Ji, X. Li, Numerical analysis on the energy performance of the PCMs-integrated thermochromic coating building envelopes, Build. Environ. 233 (2023) 110113, https://doi.org/10.1016/j.buildenv.2023.110113.
[47] A. Kitsopoulou, E. Bellos, P. Lykas, C. Sammoutos, M.G. Vrachopou-los, C. Tzivanidis, A systematic analysis of phase change material and optically advanced roof coatings integration for Athenian climatic conditions, Energies 16 (22) (2023) 7521, https://doi.org/10.3390/en16227521.
[48] E. Crespo Sánchez, D. Masip Vilà, Thermochromic materials as passive roof technology: their impact on building energy performance, Energies 15 (6) (2022) 2161, https://doi.org/10.3390/en15062161.
[49] M. Zinzi, S. Agnoli, G. Ulpiani, B. Mattoni, On the potential of switching cool roofs to optimize the thermal response of residential buildings in the Mediterranean region, Energy Build. (2021) 233, https://doi.org/10.1016/j.enbuild.2020.110698.
[50] A.A. Butt, S.B. de Vries, G.M. Loonen, J.L. Hensen, J. Stuiver, B.S. van den Ham, J. F. Erich, Investigating the energy-saving potential of thermochromic coatings on building envelopes, Appl. Energy (2021) 291, https://doi.org/10.1016/j.apenergy.2021.116788.
[51] J. Hu, X.B. Yu, Adaptive building roof by coupling thermochromic material and phase change material: energy performance under different climate conditions, Constr. Build. Mater. (2020) 262, https://doi.org/10.1016/j.conbuildmat.2020.120481.
[52] V. Granadeiro, M. Almeida, T. Souto, V. Leal, J. Machado, A. Mendes, Thermochromic paints on external surfaces: Impact assessment for a residential building through thermal and energy simulation, Energies 13 (8) (2020) 1912, https://doi.org/10.3390/en13081912.
[53] C. Fabiani, V.L. Castaldo, A.L. Pisello, Thermo-chromic materials for indoor thermal comfort improvement: finite difference modeling and validation in a real case-study building, Appl. Energy (2020) 262, https://doi.org/10.1016/j.apenergy.2019.114147.
[54] J. Hu, X.B. Yu, Thermo and light-responsive building envelope: energy analysis under different climate conditions, Solar Energy 193 (2019) 866–877, https://doi.org/10.1016/j.solener.2019.10.021.
[55] C. Fabiani, A.L. Pisello, E. Bou-Zeid, J. Yang, F. Cotana, Adaptive measures for mitigating urban heat islands: the potential of thermochromic materials to control roofing energy balance, Appl. Energy 247 (2019) 155–170, https://doi.org/10.1016/j.apenergy.2019.04.020.
[56] U.S. Department of Energy (DOE), Application Guide for EMS, 2022.
[57] American Society of Heating, Refrigerating and Air-Conditioning Engineers, ASHRAE 90.1- Energy Standard for Sites and Buildings Except Low-Rise Residential Buildings, 2022.
[58] Associação Brasileira de Normas Técnicas, ABNT - NBR 15220: Desempenho Térmico de Edificações, 2005. Rio de Janeiro.
[59] C.S. Amore, L.Z. Shimbo, M.B.C. Rufino, My House... and the City. Evaluation of the "Minha Casa, Minha Vida" Program in Six Brazilian States, Letra Capital, Rio de Janeiro, 2015.
[60] M.M. Rossi, A.P.O. Favretto, C. Grassi, J. DeCarolis, S. Cho, D. Hill, K.M.S. Chvatal, R. Ranjithan, Metamodels to assess the thermal performance of naturally ventilated, low-cost houses in Brazil, Energy Build. 204 (2019) 109457, https://doi.org/10.1016/j.enbuild.2019.109457.
[61] Instituto Nacional de Metrologia, Normalização e Qualidade Industrial, INMETRO – Anexo geral V – Catálogo de propriedades térmicas de paredes, coberturas e vidros. Anexo da portaria INMETRO, 2013, p. 50, n°.
[62] Associação Brasileira De Normas Técnicas, ABNT - NBR 15575: Edificações habitacionais – Desempenho, 2021. Rio de Janeiro.
[63] M.K. Bracht, M.S. Olinger, A.F. Krelling, A.R. Gonçalves, A.P. Melo, R. Lamberts, Multiple regional climate model projections to assess building thermal performance in Brazil: understanding the uncertainty, J. Build. Eng. 88 (2024) 109248, https://doi.org/10.1016/j.jobe.2024.109248.
[64] D. Shi, C. Zhuang, C. Lin, X. Zhao, D. Chen, Y. Gao, R. Levin-son, Effects of natural soiling and weathering on cool roof energy savings for dormitory buildings in Chinese cities with hot summers, Solar Energy Mater. Solar Cells 200 (2019) 109954, https://doi.org/10.1016/j.solmat.2019.109954.
[65] A.C.H. Araujo, Solar Absorptance and the Natural Aging of Roof Tiles Exposed to Weather, Institute of Architecture and Urbanism, University of São Paulo, São Carlos, 2022, https://doi.org/10.11606/D.102.2022.tde-06062022-143613. Master's Thesis.